MNRAS **000**, 1–10 (2020) Preprint 14 September 2020 Compiled using MNRAS LaTeX style file v3.0

Spectroscopic and photometric time series of the bright RRc star T Sex

József M. Benkő[1,2]*, Ádám Sódor[1,2] and András Pál[1]
[1] *Konkoly Observatory, Research Centre for Astronomy and Earth Sciences, Konkoly Thege M. u. 15-17., H-1121 Budapest, Hungary*
[2] *MTA CSFK Lendület Near-Field Cosmology Research Group*

Accepted XXX. Received YYY; in original form ZZZ

ABSTRACT

We present spectroscopic time series observations on one of the brightest northern RRc star, T Sex. In addition to these, we also analysed massive photometric data sets, particularly the recent observations of the *TESS* space telescope. The main findings of our studies are as follows: T Sex, unlike all RRc stars whose space photometry has been analysed, shows only the $0.5 f_x$ frequency as an additional pulsation frequency. With this, T Sex may be the first member of a rare group of RRc stars identified by space photometry. The spectroscopic data show a periodic distortion of the Hα line with the pulsation phase. This phenomenon has not been reported for any RRab stars. The characteristic line distortion is probably caused by the turbulent convection, which resulted in higher macroturbulent velocity for T Sex than for a typical RRab stars. Line doubling of the Na D line was observed between the 0.37 and 0.80 pulsation phases. The explanation of this phenomenon is that the two absorption components originate from different sources. The redder component comes from the pulsating atmosphere of the star, while the bluer one from the interstellar space. At phase 0.438 we detected emission on the Na D line, which may indicate a weak shock wave.

Key words: stars: oscillations – stars: variables: RR Lyrae – stars: individual: T Sex – methods: data analysis – space vehicles

1 INTRODUCTION

Variable stars are typically investigated by using photometric time series. Spectroscopic and, in particular, spectroscopic time series analysis are less frequent. It has practical reasons; spectroscopy is generally a more "expensive genre". For a given star spectroscopy requires a larger telescope, more complex and more expensive equipment than photometry. This general difficulty is even more serious for RR Lyrae stars because their relatively faint apparent magnitudes ($m_V > 7.45$ mag), short periods (0.3 – 0.7 d) and non-sinusoidal light variations limit the feasible integration time. The actual situation was well described by Jurcsik et al. (2017): "Complete radial velocity curves were published for less than 50 Galactic field RR Lyrae stars and less than 10 RR Lyraes in globular clusters previously." The circumstances, however, are gradually changing as modern echelle spectrographs become more and more prevalent. These powerful tools provide useful data on RR Lyrae stars even with relatively small telescopes. This is demonstrated nicely by some recent spectroscopic time series studies (e.g. Chadid et al. 2017; Sneden et al. 2017; Gillet et al. 2019).

Spectroscopic time series studies of RRc stars – RR Lyrae pulsating in their first overtone mode – are even less frequent than studies of fundamental-mode pulsator RRab stars, though RRc stars are by no means less interesting objects. A surprising new phenomenon has been discovered in all of these stars by analysing *Kepler* and *CoRoT* space photometric data: they all appear to be pulsating in additional modes (Moskalik 2013; Moskalik et al. 2015; Szabó et al. 2014; Sódor et al. 2017). The period ratio of these additional modes with the dominant (overtone) one P_x/P_1 are always in a narrow range around 0.61 or 0.63. Soon, further additional modes were also found in ground-based observations of some RRc stars at period ratios of 0.68 (Netzel et al. 2015) and 0.72 (Prudil et al. 2017). On the basis of his simplified model calculations, Dziembowski (2016) suggested that the additional frequencies of the first two groups ($P_x/P_1 \sim 0.61$, $P_x/P_1 \sim 0.63$) might be associated with $l = 8$ or $l = 9$ non-radial modes. The nature of the other two groups are still mysterious. We have to stress that such kind of additional modes have never been detected in any of the RRab stars. Additional modes were also discovered in RRab stars, but at different period ratios, and those have different explanations.

These new phenomena have drawn our attention to RRc stars. Since space photometric results suggested that each RRc star shows extra modes, the target selection appeared to be an easy task. According to Maintz (2005), only six RRc star are known in the northern sky brighter than ten visual apparent magnitude. The brightest one (V764 Mon, $V_{\max} = 7.13$ mag) is even brighter than RR Lyr itself. So we focused on this star but we also selected another, slightly fainter star, T Sex ($V_{\max} = 9.81$ mag) as secondary target in the

---

* E-mail: benko@konkoly.hu

Table 1. Log of T Sex spectroscopic observations

Night (yyyy-mm-dd)	JD (-2 400 000)	$\langle S/N \rangle$	ϕ	n
2015-03-05	57087	11	0.606-0.732	2
2015-03-07	57089	51	0.003-0.932	14
2015-03-10	57092	19	0.020-0.945	7

observing window of V764 Mon. We sought to achieve the most complete pulsation-phase coverage with the shortest possible integration times for both stars.

A quick look at the spectra revealed that V764 Mon is not, in fact, an RR Lyae, but a fast-rotating δ Scuti star. The results about this star will be published elsewhere. In this paper, we study T Sex, which is a bona fide RRc pulsator.

2 OBSERVATIONS AND REDUCTION

2.1 Photometric data

Two sufficiently extensive photometric time series were analysed. The ASAS-3 V band data (All Sky Automated Survey, Pojmański et al. 2005) contains 504 observed data points. Before the analysis, the outlying points fainter than 10.4 mag and the less accurate observations flagged by 'D' in the catalogue had been removed. In the end, 457 data points remained.

Up to the time of writing of this manuscript, the *TESS* space mission (Ricker et al. 2015) observed T Sex once, in Sector 8, obtaining 17 755 data points. The observation of Sector 8 was taken in February 2019 almost continuously, covering 24.62 days with 2 min exposures. This exposure time represents oversampled high-cadence observations[1].

From the data offered by the archive, the light curves obtained from the corrected aperture photometry (PDCSAP) fluxes were used for this analysis, and only the best-quality data (marked with a quality flag 0) were used, which corresponds to 13 395 data points. The fluxes were transformed to a magnitude scale. We mention that *TESS* magnitudes (zero point, the amplitude and the errors) are scaled with the reference magnitude. We accepted the value of m_{TESS} = 9.779 mag according to the TESS data release. The typical error of the individual photometric data points is ~ 0.0013 mag.

2.2 Spectroscopic data

For the observations we used the ACE fibre-fed échelle spectrograph attached to the 1-m RCC telescope at the Piszkéstető mountain station of the Konkoly Observatory. The spectra cover the 4150-9150 Å wavelength range with a resolution of R ≈20 000. A total of 23 spectra were recorded from the target star on three nights between 5 and 10 March 2015 (Table 1). The integration time was 30 min, which is a good trade off between getting enough pulsation phase resolution and reaching acceptable signal-to-noise ratio (see column 4 in Table 1 for nightly averaged S/N values estimated by iSpec (Blanco-Cuaresma et al. 2014; Blanco-Cuaresma 2019)).

The ACE spectra were reduced using standard IRAF (Tody 1986, 1993) tasks including bias, dark and flat-field corrections, aperture extraction, and wavelength calibration using thorium-argon calibration images which were taken after every third object frames. The normalisation, cosmic-ray filtering, order merging were performed by our PYTHON scripts (developed by ÁS). Each spectrum was also corrected to the barycentric frame. The processed spectra are attached to this paper as an electronic supplement.

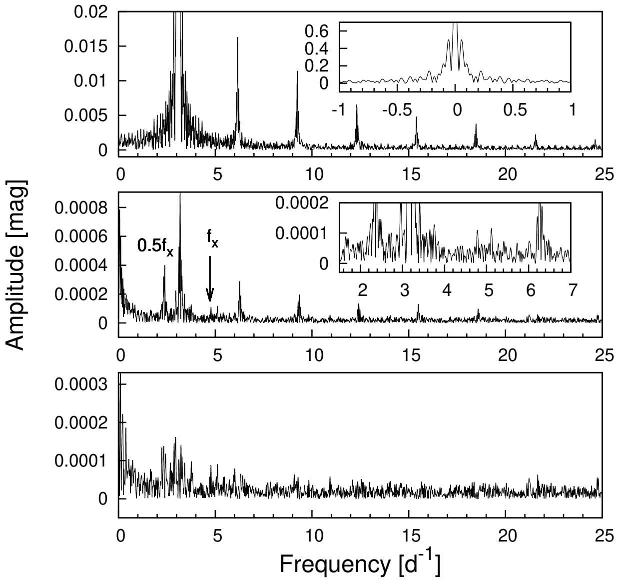

Figure 1. Fourier spectra of the *TESS* data on T Sex during the subsequent pre-whitening steps. The original spectrum (top panel) and the central part of the window function (inset in top panel), the spectrum after pre-whitening the data with the main pulsation frequency f_1 and its 16 harmonics (middle). The inset in the middle panel is the expansion of the frequency range around $0.5f_x$ and f_x. Bottom panel: residual after pre-whitening the spectrum shown in the middle panel with eight further significant frequencies. To make the harmonic structure more apparent, the amplitude limit on the top panel is lower than the amplitude of the main frequency (0.08 mag).

3 ANALYSIS OF THE PHOTOMETRIC DATA

Although this work focuses on spectroscopic time series observations of T Sex, we also needed some photometric data for determining the proper period and phases. Furthermore, the analysis of the photometric data yielded an unexpected result, too.

The ASAS data set was analysed by using the Fourier fitting tool of the Period04 package (Lenz & Breger 2005). Since these data points spread over 9 years (3276 days between December 2000 and November 2009), the Nyquist frequency (~0.24 d^{-1}) is significantly lower than the pulsation frequency (f_1=3.0798 d^{-1}), and the Fourier spectrum had to be calculated well above this limit frequency. Consequently, the resulting spectrum has a periodic structure. It contains the main frequency, its daily alias frequencies and the annual frequency caused by the seasonality of the observations with its daily aliases. The 1-year frequency also occurs in side peaks around the main frequency. Apart from the pulsation frequency, no additional frequency can be detected above the noise level (~ 0.04 mag).

The Fourier spectrum of the *TESS* data shows the main pulsation frequency (f_1=3.079 d^{-1}) and its harmonics (see top panel in Fig. 1). We pre-whitened the data with f_1 and its all 16 significant harmonics up to the Nyquist frequency (50.0 d^{-1}). The residual

---

[1] The data are publicly available at the Mikulski Archive for Space Telescopes: `https://mast.stsci.edu/portal/Mashup/Clients/Mast/Portal.html`

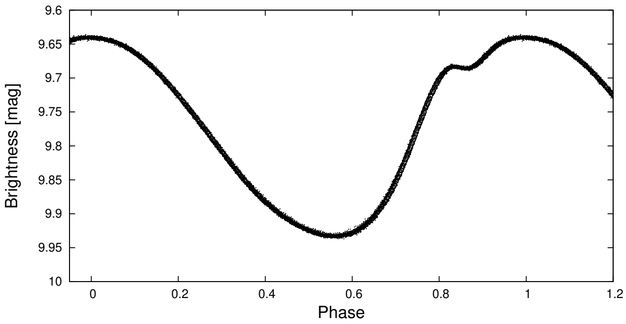

Figure 2. Phased light curve of T Sex observed by *TESS* satellite.

Table 2. Sample part of the radial velocity data tables. The columns contain the barycentric Julian date (BJD), the measured radial velocity $v_{\rm rad}$, its uncertainty $\sigma(v_{\rm rad})$ and the corresponding pulsation phase ϕ.

BJD (d)	$v_{\rm rad}$ (km s^{-1})	$\sigma(v_{\rm rad})$ (km s^{-1})	phase
(...)			
2457089.25160	22.87	1.67	0.634659
2457089.27272	28.37	1.95	0.699704
2457089.29368	31.76	3.38	0.764256
2457089.32674	35.25	1.60	0.866074
2457089.34768	37.48	2.31	0.930565
(...)			

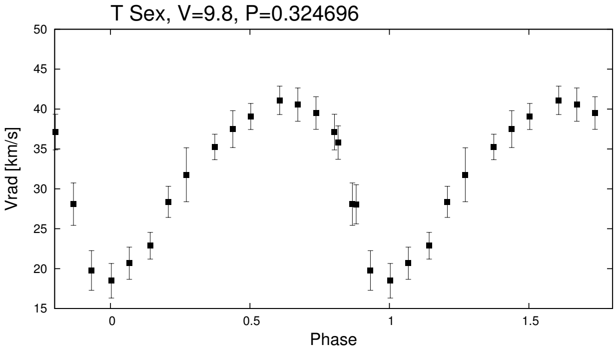

Figure 3. Radial velocity curve of T Sex. The error bars show the 1σ calculated formal errors (around 1-2 km s^{-1}).

spectrum is shown in the middle panel of Fig. 1. Eight significant peaks can be detected in this residual. Six of them can be written in the form $kf_1 + f^{(1)}$, where $k = 1, 2, \ldots 6$, and $f^{(1)} = 0.103$ d^{-1}, moreover $f^{(2)} = 0.055$ and $f^{(3)} = 2.3919$ d^{-1}. All but one of these frequencies are of instrumental origin. The window function (inset in top panel of Fig. 1) contain the data length frequency ($f^{(2)} = 0.055$ d^{-1}). We can now identify $f^{(1)} \approx 2f^{(2)}$. These identifications are within the frequency errors because the short *TESS* data set the Rayleigh frequency resolution is rather low (0.04 d^{-1}).

The only significant ($S/N = 5.7$) non-technical frequency is $f^{(3)}$. As mentioned in the introduction, all the space photometric measurements made from RRc stars and that have been studied show additional frequencies. The Fourier spectra of those stars typically contain a strong peak (f_x), the ratio of which to the main period f_1 is around 0.61 or 0.63, as well as its harmonics and linear combinations with f_1, respectively. In some cases the sub-harmonic $0.5f_x$ is also detectable (*CoRoT* Szabó et al. 2014, *Kepler/K2* Moskalik et al. 2015; Molnár et al. 2015; Sódor et al. 2017).

According to Dziembowski (2016), signals at sub-harmonic frequencies $0.5f_x$, are the real frequency of the non-radial modes of degrees $l = 8$ and $l = 9$, and the signals at f_x are harmonics. Because of cancellation effects, generally the harmonics can easier be observed than the mode frequency itself. On the large OGLE RRc sample, Netzel & Smolec (2019) showed recently that the longer-ratio sequence ($P_x/P_1 \sim 0.63$) belongs most probably to the $l = 8$ mode. Stars pulsating in this mode tend to show both f_x and $0.5f_x$ frequencies as well. From the 960 stars in which an additional mode was found by Netzel & Smolec (2019), $0.5f_x$ was also detected for 114 stars and even in 35 cases (3.6%), this frequency had larger amplitude than that of f_x.

If we identify $f^{(3)}$ as $0.5f_x$ then $f_x = 4.7826$ d^{-1} and $f_1/f_x = 0.643$. This ratio is higher than the median of the 0.63 sequence but within the observed range of this ratio. Such identification of $f^{(3)}$ is likely because a peak, although not significant ($S/N = 3.2$), is indeed visible at the position of the calculated f_x (see the inset in middle panel of Fig 1). Near to this one, at $f^{(4)} = 5.1132$ d^{-1}, we can also see a peak of similar amplitude ($S/N = 3.1$). The ratio of this frequency ($f_1/f^{(4)} = 0.602$) suggests that it might be the harmonic of the $l = 9$ mode. That is, T Sex contains both $l = 8$ and $l = 9$ mode pulsations as well. This is rather common phenomenon, Netzel & Smolec (2019) found this in more than 10% of their sample.

By removing the eight significant frequencies discussed above with a subsequent pre-whitening step, the residual spectrum shown in the bottom panel of Fig. 1 is obtained. No further significant ($S/N > 4$) frequency can be detected in this spectrum.

The pulsation period obtained from the *TESS* data ($P_1 = 0.3248 \pm 0.004$ d) is in agreement with the more precisely defined ASAS period ($P_1 = 0.324696 \pm 0.00003$ d). The *TESS* light curve folded with the ASAS period is shown in Fig. 2. Since the standard deviation of the curve is very small, no phase-shifted cycles are seen, it is likely that the period between the end of the ASAS measurements (2009) and the beginning of the TESS measurements (2019) did not change significantly.

4 RADIAL VELOCITY CURVE

We determined the radial velocity curve of T Sex. The radial velocities were calculated by cross-correlating the spectra with a metallic line mask containing 622 metallic lines between 4800 and 5600 Å. We used Gaussian fitting functions for determining the radial velocities and their uncertainties from the the cross-correlation functions.

The S/N ratio in the cross-correlation functions are 80 – 150, which provide a precision of ~1 – 2 km s^{-1} for the radial velocities. The systematic errors resulted in the data processing and the stability of the wavelength calibration system of the ACE instrument are better than 0.36 km s^{-1}, based on observations of radial velocity standards (Derekas et al. 2017). The radial velocity curves are published as electronic tables. The structure of these tables is shown in the excerpt in Table 2.

We used here the ASAS-3 period determined above in Sec. 3, For zero phase of the radial velocity curve we simple used the ephemeris belonging to the ASAS photometric maxima because these two values are coincident within the observation error (Jurcsik et al. 2015, 2017; Sneden et al. 2017). The exact ephemeris was not critical in this study. The obtained radial velocity phase curve in Fig. 3 demonstrates well the complete phase coverage of our observations.

Although T Sex is one of the brightest RRc stars, up to now only four radial velocity curves were published (Tift & Smith 1958; Preston & Paczyński 1964; Barnes et al. 1988; Sneden et al. 2017) and phase coverage of these curves are complete only in Tift & Smith (1958) and Barnes et al. (1988). By using the zero point of a four-element Fourier fit to the radial velocity curve we determined the mean velocity as $v_0 = 31.7 \pm 0.5$ km s^{-1}. This mean velocity is approximated the velocity of the stellar rest frame with respect to the solar system barycenter (v_γ). Strictly speaking, however, this is not completely true, because the optical depth changes during the pulsation. The radial velocity curve does not represent any physically moving fluid element (e.g. Karp 1975). However, the so-called k-term – the difference between v_γ and v_0 – must be less than 2 km s^{-1} for RRc stars. This value was found for more extended atmosphere of Cepheids by Nardetto et al. (2008).

Our mean velocity value is 6.5 km s^{-1} higher than the latest published in the literature ($v_0 = 25.2 \pm 1$ km s^{-1}, Gontcharov 2006). This latter mean radial velocity compilation, however, is prepared for Galactic kinematic purpose and optimised for non-variable stars. As Kollmeier at al. (2013) showed, the mean radial velocity of RRc stars can be well estimated by measuring the radial velocity curve at the phase of $\phi = 0.32$. By a simple interpolation we obtain $v(0.32) = 33.5 \pm 2.4$ km s^{-1}. This value is consistent within 1σ with our previous calculation and the recent measurements of Sneden et al. 2017. (They did not calculated v_γ for T Sex because of their incomplete phase coverage, but from their data we found $v(0.32) = 28.6 \pm 2.5$ km s^{-1}.)

5 SPECTRAL VARIATIONS WITH PULSATION PHASES

5.1 Hydrogen Hα line

Our spectra cover the hydrogen Balmer Hα, Hβ and Hγ lines. Since the detector is more sensitive in redder wavelengths, Hα lines have the highest S/N ratio among the Balmer series. Therefore we investigated the motions and line-profile variations of the Hα line over the pulsation phase.

In Fig.4, the Hα line-profile variations of T Sex on the best night (2015-03-07) are plotted in the stellar rest frame. To make the phase dependence easier to follow, the normalised spectra are shifted vertically with phase dependent constants. The thin grey curves represent the original spectra. Since these spectra show many weak (mostly telluric) lines and some noise we plot smoothed spectra as well (black curves in Fig.4). The latter are better for following line profile variations.

If we look at the line positions, we find periodic shifts in the stellar rest frame: The Hα line is blueshifted between phases $\phi \sim 0.87 - 0.21$ and redshifted between $\phi \sim 0.37 - 0.74$. These variations are the natural consequence of the radial pulsation motion in which the hydrogen-absorbing layer is involved and defines a radial velocity curve slightly different from the one obtained from metallic lines. These differences are discussed in detail by Sneden et al. (2017).

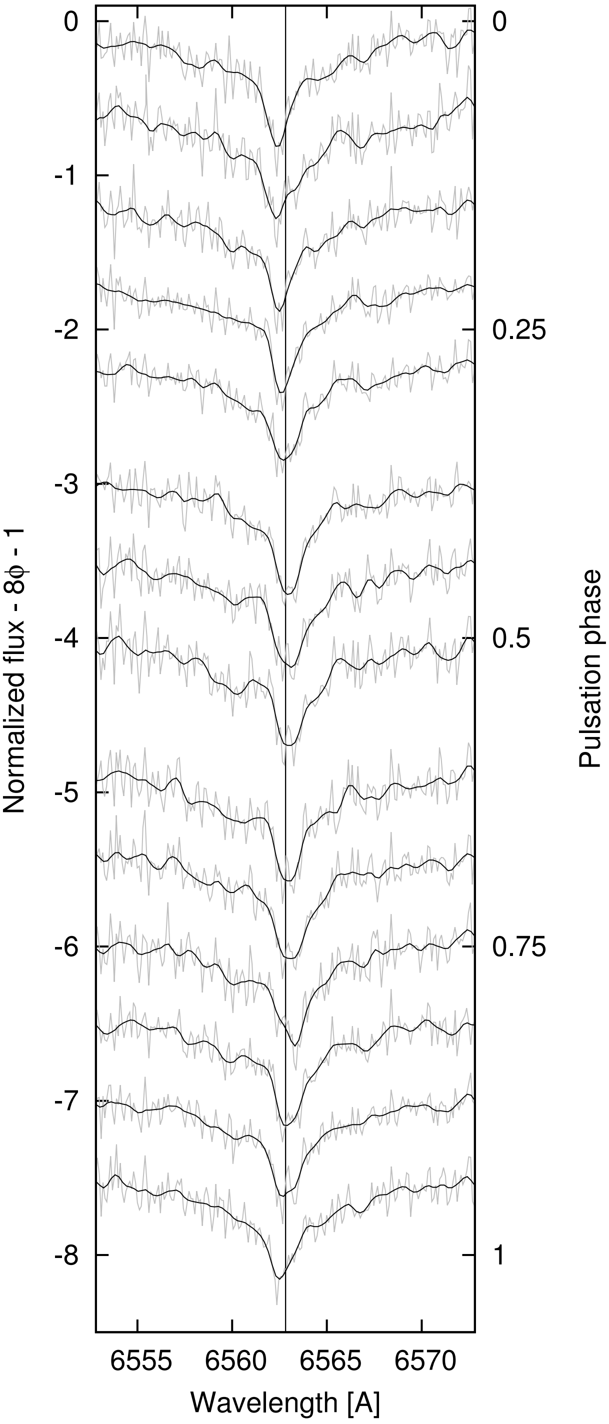

Figure 4. Hα line variations of T Sex over the pulsation cycle in the stellar rest frame. The normalised spectra are shown with thin grey line. The black curves are the smoothed spectra. Vertical line marks the laboratory position of the Hα line.

5.2 Periodic line-profile distortions

The Hα line, however, does not simply shift periodically around the laboratory wavelength corrected with the center-of-mass velocity, but its profile also changes with the pulsation phase. In Fig. 5, we show two highly asymmetric phases compared with a symmetric

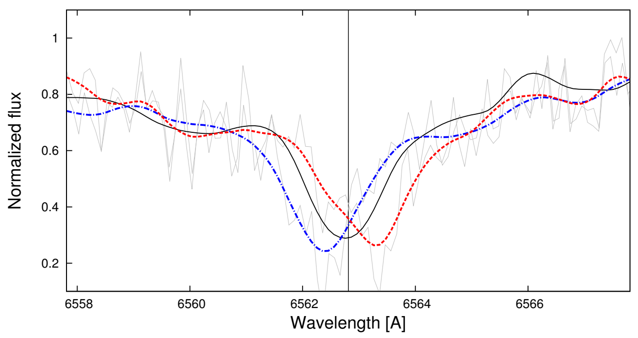

Figure 5. Hα line-profile distortions of T Sex over the pulsation cycle. The normalised spectra are shown with thin grey lines. The black continuous curve shows a smoothed spectrum at $\phi = 0.607$ with symmetric line profile corrected with its relative velocity (9.39 km s^{-1}) to the stellar rest frame. The blue dash-dotted curve is a blue shifted asymmetric spectrum at $\phi = 0.003$ while the red dashed curve shows the red shifted asymmetric spectrum at $\phi = 0.737$. The vertical line indicates the laboratory position of the Hα line.

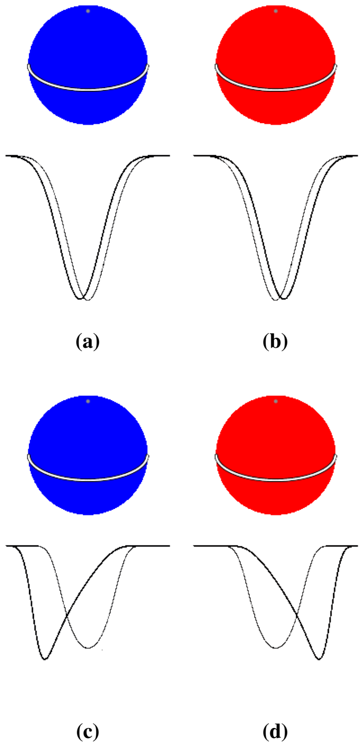

Figure 6. Extreme cases of line profile variation on a radially pulsating star with the parameters of a typical RRc stars. The figures were prepared by using NRP Animation Creator. The subfigures a) and c) show maximal contraction b) and d) maximal expansion phases. In the top row $v \sin i$ = 1 km s^{-1}, in the bottom row $v \sin i$ = 15 km s^{-1}.

one. Such line-profile variations has not been reported for RRc stars before.

This line asymmetry is a remarkable difference compared to the variation of Hα line of RR Lyrae. In that case an Hα line doubling can be detected between $\phi = 0.943$ and $\phi = 1.027$ but the core of the line remains symmetric for all phases (Gillet et al. 2019). Additionally, some metallic lines of RR Lyrae also show phase dependent profile distortions around the brightness maxima ($\phi \sim 0.91 - 0.97$) and the strength of this effect depends on the Blazhko phase (Chadid & Gillet 1996, 1997). These two phenomena have been explained by the same physical mechanism: a hydrodinamical shock wave passing through the pulsating atmosphere causing two distinct absorbent layers (Schwarzschild 1952; Fokin & Gillet 1997). In this case, the asymmetric metallic lines would be nothing more than overlapping double lines.

The Hα line doubling and the asymmetry of metallic lines in RRab stars appear only around the phase of maximum brightness. The phenomenon presented here is more similar to that observed in some metallic lines of classical Cepheids and β Cep stars (Nardetto et al. 2008, 2013). Nardetto et al. (2008) discussed three explanations for the effect. The time- and wavelength dependence of the limb-darkening within the spectral lines, velocity gradients in the atmosphere and the relative motion of the line-forming region with respect to the corresponding mass elements. The third explanation is closely related to the one that was mentioned for RRabs. Nardetto et al. (2008) concluded that for quantitative modelling of line asymmetries, a detailed hydrodynamic model, in which convection is taken into account, should be combined with a wavelength-dependent radiative code.

5.2.1 Phenomenologic explanation

Pulsating atmospheric models that take into account both convection and shock waves and are able to compute synthetic lines profiles for Cepheids or RR Lyrae stars have not yet been developed. There is, however, a smart tool NRP Animation Creator (NRPAC)[2] (Schrijvers et al. 1997; Telting & Schrijvers 1997; Schrijvers & Telting 1999) that allows us to model line profile variations of pulsating stars. The program is optimised for fast rotating non-radially oscillating stars, such as δ Scutis and related stars. Because of its assumptions (e.g. adiabatic pulsation) it is not suitable for quantitative analysis of line-profile variations in an RR Lyr pulsator. Nonetheless, if we assume a radially pulsating ($l = m = 0$) star with the parameters of a typical RRc star (mass $M = 0.65\ M_{\odot}$, radius $R = 4\ R_{\odot}$, 3D velocity amplitude $A(v)$=20 km s^{-1}, pulsation frequency f_1=0.3 d^{-1}, $v \sin i$ = 15 km s^{-1}), we can qualitatively reproduce the observed line-profile distortions.

Fig. 6 shows the line profile of two extreme phases (the maximal contraction in the left side, and the maximal expansion in the right) of a radially pulsating star. The line profiles of the resting stars are shown by thin lines. The same parameters were used for all the plots, except for $v \sin i$. We used $v \sin i$ = 1 km s^{-1} for the top row and 15 km s^{-1} for the bottom row. For $v \sin i$ = 1 km s^{-1}, the line profile is practically not distorted and it shows similar profiles as the observed one of Gillet et al. (2019) for RR Lyrae. Fig. 6 illustrates well that the key of reproducing observed-like line profile variations of T Sex is applying a relatively high $v \sin i$ value in NRPAC.

Preston et al. (2019) summarises the present knowledge of RR Lyrae axial rotation and macroturbulence which are generally

---

[2] `http://staff.not.iac.es/~jht/science/nrpform/`

hard to separate because these two phenomena broaden the line profiles in a similar fashion. Preston et al. (2019) found an upper limit for the macroturbulent velocity of RRab stars as 5 ± 1 km s^{-1}. They also showed that this velocity is less uniform for RRc stars and it could be as high as $\sim$ 12 km s^{-1}.

As we have seen, reproducing the line-profile variations of T Sex with NRPAC requires a sufficiently large $v \sin i$. This tool, however, does not use the macroturbulent velocity as a free parameter, therefore the suggested high $v \sin i$ does not necessary mean a high equatorial rotation speed, but could imply a more intense macroturbulence caused by the convection. This finding agrees with the theoretical calculations of Gautschy (2019), showing the more significant role of atmospheric convection in RRc stars than in RRab stars. It means, on the one hand, that convection is more important in the energy transport and, on the other hand, that, unlike RRab stars, it is present in almost all pulsation phases.

5.2.2 Spectral fitting

We also tried a more quantitative estimation for macroturbulent velocity by fitting theoretical stellar model atmospheres to the observed spectra. Following Sneden et al. (2017), we prepared a good S/N combined spectrum from the best 16 spectra, which samples the complete pulsation cycle almost evenly. Then we shifted each of them with the corresponding radial velocity and computed the median spectrum. The vicinity of the Mg triplet (between 5165 and 5190 Å) of the median spectrum is shown in Fig. 7 with black dots. We fitted theoretical spectra to this median spectrum by minimizing χ^2.

We calculated the atmospheric parameters of T Sex from this region using the ‘Synthetic spectral fitting’ tool of iSpec. After trying several radiative transfer codes (SPECTRUM, Turbospectrum, MOOG) integrated into the iSpec package, we concluded that there is not much difference in the obtained fits in our case, so the integrated SPECTRUM radiative transfer code (Gray & Corbally 1994) and MARCS GES model atmospheres (Gustafsson et al. 2008) were selected. The solar abundance of Grevesse et al. (2007) and GES (Gaia-ESO Survey) atomic line list (Heiter et al. 2015) were used.

Several test runs showed that the parameters of Sneden et al. (2017) obtained from the phase-averaged spectrum agrees within the errors with the results from our median spectrum, therefore, we accepted and fixed them. We obtained $T_{\rm eff}$ = 6958 K effective temperature, $\log g$ = 2.12, [M/Fe]=−1.48 metallicity and [α/Fe]=0.51 alpha-element enhancement. However, we use our higher value for the microturbulence (ξ = 3.8 ± 0.6 km s^{-1}) because it always resulted in better spectral fits than ξ = 2.3 km s^{-1} of Sneden et al. (2017).

The macroturbulence $v_{\rm mac}$ and the projected rotational velocity $v \sin i$ lead to similar line broadening effects, as Preston et al. (2019) showed, and it is difficult to separate them. We arrived at the same conclusion here. A similarly accurate fit can be achieved either with $v \sin i = 0$, $v_{\rm mac}$ = 23 km s^{-1} or with $v \sin i = 15$, $v_{\rm mac}$ = 0 km s^{-1}, respectively. Since RR Lyrae stars are slow rotators, it is very likely that the first case is closer to reality. This fit is shown by a red line in Fig. 7.

Although in a completely different way, we arrived at the same result as before from studying the variations in the Hα line: either $v \sin i$ or rather $v_{\rm mac}$ is relatively large ($\sim$15-20 km s^{-1}). This supports our phenomenological explanation of the periodic line distortions.

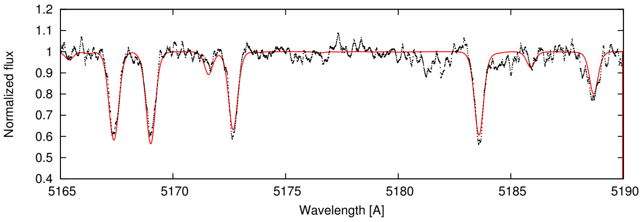

Figure 7. Spectral fit for the Mg triplet range of T Sex. The small black dots show the median spectrum over the whole pulsation cycle. The red continuous line shows the best-fitting synthetic spectrum.

5.3 Sodium lines

5.3.1 Line doubling

In Fig. 8 we show the Na I D line-profile variations of T Sex over the pulsation cycle. In the left panel the spectra are plotted in a system co-moving with the pulsation, that is, the instantaneous radial velocity was subtracted from each spectrum. In other words, this system moves with the average pulsation motion of the atmosphere defined by the radial velocity curve in Fig. 3. It can be seen that the D_1 and D_2 line profiles are rather similar in all phases: they show significant deviation from a single Gaussian profile between the phases of $\phi \approx 0.28$ and $\phi \approx 0.88$. The distortion becomes line doubling between $\phi \approx 0.37$ and $\phi \approx 0.80$. The phenomenon is observable over 60% of the pulsation cycle.

Line doubling of the sodium D lines in the spectrum of a fundamental mode pulsating RRab star (RR Lyr itself) was reported for the first time by Gillet et al. (2017), who found this line doubling to be coincided with an Hα emission of RR Lyr at the phase $\phi \approx 0.227$. In a more recent and detailed study, Gillet et al. (2019) showed that the D_1 line is doubled over 75% of the pulsation cycle. The position of the redder component is fixed during the whole pulsation cycle within the stellar rest frame, therefore this component was explained by interstellar origin.

Our present study shows line doubling phenomenon in an overtone pulsating RRc star. As we seen in the left-hand panel of Fig. 8, the position of the red part of the line is fixed with respect to the co-moving frame that is it follows the atmospheric motions which are represented by the radial velocity curve and obtained from the averaged motions of metallic lines. Thus, it can be assumed that the atmospheric layer where this line is formed is at or nearby the layer where the metallic lines taken into account in the calculation of the radial velocity curve are formed.

The position of the blue component in the left panel of Fig. 8 varies with the phase but this is a virtual variation. When we construct the spectral variations over the pulsation cycle within a rest of frame of the center-of-mass of T Sex (right panel of Fig. 8), we see that actually the position of the blue component is fixed. In other words this component does not share the motion of the pulsating atmosphere.

What is the origin of these ‘fixed’ components? The telluric origin is unlikely because the known telluric absorption lines in this spectral region (see e.g. Hobbs 1978) are weak and they have complex fine structure which has not been detected. Circumstellar and interstellar origin are the two natural potential explanations. According to Gillet et al. (2019), the +50.3 km/s velocity interstellar line they found in the spectra of RR Lyr may originate from the wall of the Local Bubble (Frisch et al. 2011). This explanation applies for our case as well. The recent 3D-map of the interstellar

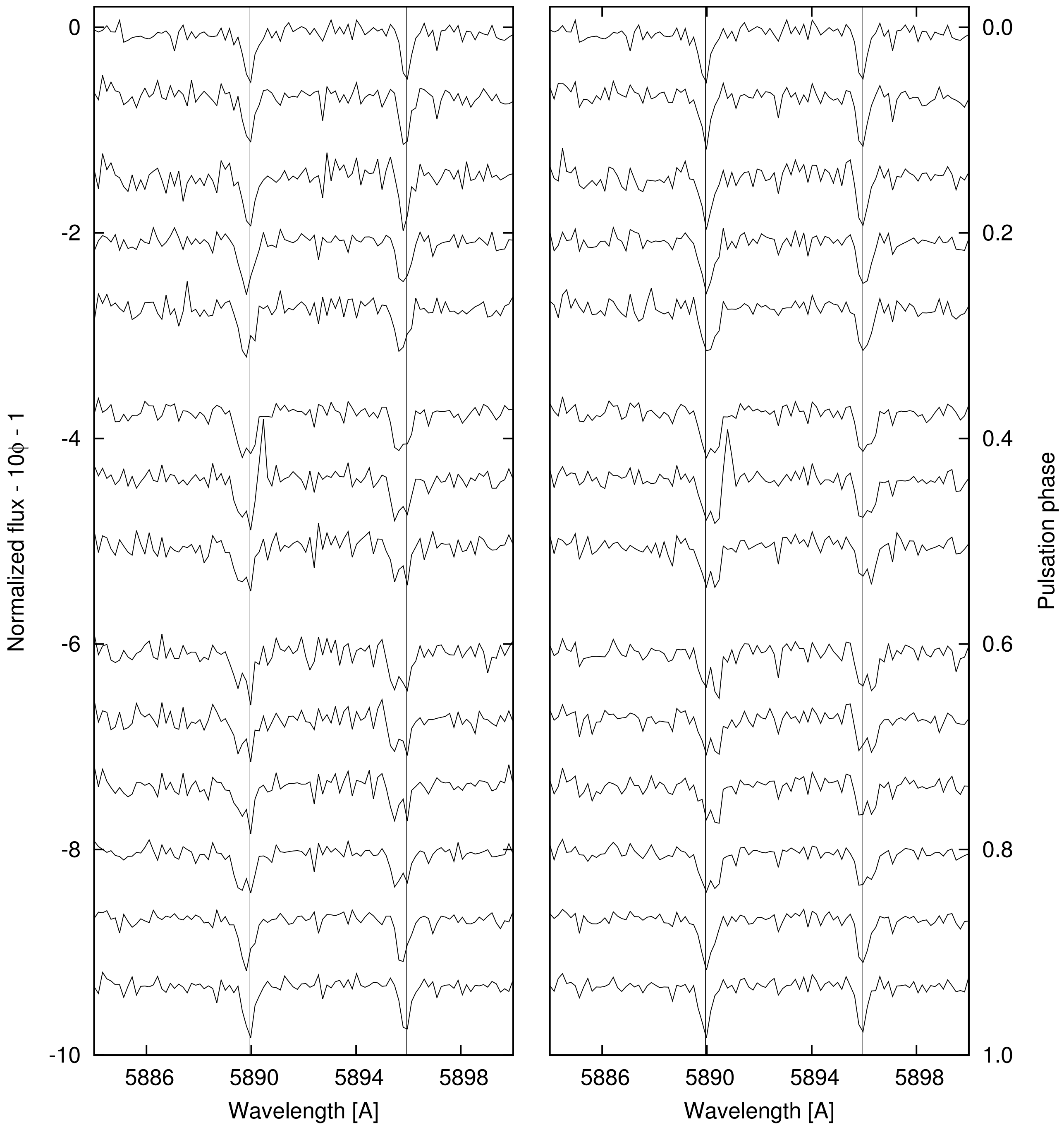

Figure 8. Sodium line variations of T Sex over the pulsation cycle in a system co-moving with the pulsating atmosphere (in the left) and in the stellar centre-of-mass rest frame (in the right), respectively. The smoothed and normalised spectra are shifted vertically according to the pulsation phase. The thin vertical lines indicate the laboratory wavelengths of the Na D_1 and D_2 lines. Spectra in the right-hand panel are shifted with the radial velocity of the stellar centre-of-mass ($-13.2\ \mathrm{km\,s^{-1}}$) to transform the Na D lines to the vicinity of their laboratory wavelengths. The slightly different line shapes are due to differences in the spline interpolation.

gas based on Na (and Ca) absorption observations (Vergely et al 2010; Welsh et al 2010) shows a gas cloud toward the direction of T Sex ($l = 235°38'$, $b = +40°36'$). This cloud is also part of the material that forms of the wall of the Local Bubble. Although the map includes only the 300 pc neighbourhood of the Sun, the contribution of more distant matter to the interstellar absorption is likely to be small, since T Sex have a high Galactic latitude, where we do not expect significant interstellar matter so far away.

Distinguishing between circumstellar and interstellar material is generally an observing task. We have to observe several stars that are close to the target star in space, and if we observe similar interstellar absorption in the check stars, we can conclude that these lines originate from the interstellar space. Otherwise, if only the

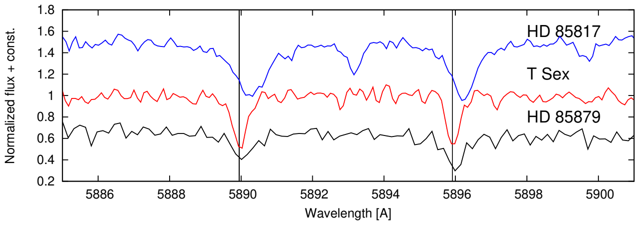

Figure 9. Spectra around the Na D lines of T Sex and two neighbouring stars; HD 85879 and HD 85817. In each case, five individual spectra were combined and equal shifts (with 18.5 kms^{-1}) were applied to transform the wavelengths of the Na lines to the laboratory values.

target shows these lines, that suggests a circumstellar origin. The method was successfully applied for discovering circumstellar discs (see e.g. Redfield 2007; Redfield et al. 2007; Rebollido et al. 2018). In the case of distant sources beyond the Local Bubble, the picture could be more complicated. As Points et al. (2004) showed, each selected star of the χ and h Per double cluster shows different Na I D absorption properties. This reflects the fine structure of the interstellar material in the line of sight. The distance of T Sex (803 ± 40 pc, from the Gaia DR2 Gaia Collaboration 2016, 2018) is much larger than the wall of the Local Bubble (~ 100 – 200 pc), but, due to its high galactic latitude ($l = +40°$), no significant interstellar material is expected beyond the Local Bubble.

In the spring of 2020, we observed 5 – 5 spectra of two brighter stars (HD 85879 and HD 85817) appearing close to the celestial position of T Sex, to investigate the issue. We determined their radial velocities with the same method as we described for T Sex in Sect. 4. The obtained values are 16.01 ± 0.34 kms^{-1} and 29.19 ± 0.37 kms^{-1} for HD 85879 and HD 85817, respectively. Both values are in agreement with the Gaia results (Gaia Collaboration 2018).

We selected five spectra for T Sex from those phases where there is no line doubling (between $\phi = 0.87$ and 0.14), i.e. the fixed components of the Na lines coincide with the moving components. The shift value $31.7 - 13.2 = 18.5$ kms^{-1} obtained from Fig. 8 meaning the barycentric velocity of the (interstellar) component was also applied for all three spectra. After averaging the 4-4 best S/N spectra for all three stars, the result is plotted in Fig. 9.

The wide line profiles of HD 85817 (top blue curve) do not show line doubling, only on the red wing of both lines of Na D doublet slight breaks can be suspected just in the proper position. These asymmetric profiles might be the result of a blend between the star and interstellar lines. Unfortunately, the radial velocity difference between HD 85879 and the interstellar matter is small (~ 2.5 kms^{-1}), therefore, the lines coming from the star and from the interstellar material can not be distinguished (bottom black curve). Although these control measurements did not provide a definite answer to the question, they rather support, in particular those of HD 85817, that we are dealing here with material of interstellar and not circumstellar origin.

5.3.2 P Cyg profile?

At the phase $\phi = 0.438$ T Sex shows an emission peak redwards to the red component of Na D_2 line (see Fig. 8) and it forms a P Cyg profile with the absorption line. As we have seen above this redder line component comes from the stellar photosphere. Appearance of sodium emission is remarkable because such phenomenon has not been reported for any RR Lyrae stars before.

We investigated possible sources of this emission. The first possibility was an observation or reduction error. This emission line profile is constructed by 6 data points which means that the spectral resolution is much higher than the line width. Therefore, it is highly unlikely that the line would be an incorrectly treated cosmics. Perhaps a more spacious anomaly in the CCD frame could cause this. However, as we checked it, no such discrepancies (e.g. hot column, scattered light, saturation trail) are seen in the raw observed frame. Additionally, there is no extra flux in any of the orders below and above the order which shows the line.

It is possible that the a given emission line does not come from the stars, but somewhere from the Earth's atmosphere. The peak intensity of our λ5890 line is ~72 per-cents higher than the strongest known optical telluric emission line of O I at λ5577. The intensity of telluric sodium D_2 line is much weaker 5 per-cents of this atmospheric O I emission line (Louistisserand et al. 1987). Furthermore, in the case of terrestrial origin, the phenomenon should be detected more or less continuously. These arguments make instrumental or terrestrial origin very unlikely.

Emission of a metallic line for RR Lyr stars has been completely unknown so far. Hα emission is known for three phase intervals of RRab stars. The Hα emission just before the luminosity maximum ($\phi \sim 0.89 - 0.93$) was detected long ago (Struve & Blaauw 1948; Stanford 1949). Later Gillet & Crowe (1988) found blue emission shoulder of Hα line. This emission appears around $\phi \sim 0.73$ which is the position of the 'bump' near the photometric minimum. The third emission effect: a red emission shoulder around $\phi \sim 0.18 - 0.39$ was discovered by Preston (2011).

Beyond the hydrogen emission phases of RRab stars helium emissions were also discovered by Preston (2009) in a sampling of 11 observed RRab stars. A stronger emission of He I D_3 line at λ5875.66 and a weaker emission at λ6678.16 were observed in all observed stars during rising light. A further helium emission of He II at λ4685.68 was also reported by Preston (2011).

For all of these cases, the physical explanation of the emission is similar: different shock waves in the atmospheres (see Gillet & Fokin 2014 and references therein). But similarly to the observations the theoretical efforts have also been concentrated on fundamental mode pulsating RRab stars. We were not able to find any theoretical study that investigates shock properties in RRc stars. Maybe the reason is that because of the smaller atmospheric velocities of RRc stars, no strong shocks are expected. From an observational point of view, Sneden et al. (2017) found no signs of shocks (line doubling, emission) in the spectra of 7 RRc stars, and estimated an upper limit of ~ 10 km s^{-1} for any possible atmospheric shocks. At the same time, the authors discussed the possibility of a compression wave around $\phi \sim 0.52 \pm 0.05$ where certain Hα radial velocity curves show a secondary maximum. As they mentioned, this wave would be "qualitatively similar to the shock $\mathrm{Sh}_{\mathrm{PM3}}$ of RRab stars (Chadid et al. 2014), which produces compression heating during infall."

If we look into Gautschy's latest theoretical calculations (see fig. 4 in Gautschy 2019) phase $\phi \sim 0.4 - 0.5$[3] of RRc stars corresponds to the phase where the early shock appear in the RRab stars (Hill 1972). Namely, where the luminosity functions of the cool edge and the hot edge of the He II partially ionised zones intersects. The physical meaning of this intersection is the collision between the infalling high atmosphere and the slower shrinking photosphere.

---

[3] We mention that Gautschy denotes the maximum radius by phase $\varphi = 0.0 = 1.0$ and not the maximum brightness as we use here. There is a ~ 0.68 phase shift between the two zero-points.

Based on these, our finding of Na emission in the appropriate pulsation phase both agrees with the theoretical calculations and the preliminary observational expectations. The wavelength difference between the absorption and emission components of D_2 line is 0.46 Å, giving a velocity difference of 23.4 km s^{-1}. Sodium absorption lines, along with other metallic lines, are formed practically in the photosphere. The velocity of the photosphere at this phase is 5.8 km s^{-1}. The total velocity of the supposed compression wave in the stellar rest frame is 29.2 km s^{-1}. This is almost an order of magnitude smaller than the shock wave velocities estimated for RRab stars.

There are two problems with this emission. First, why did not we observe similar emissions at line D_1? And second, why did not Sneden et al. (2017) detect it in their very good time-sampled spectra? There might be an answer to the first question: the intensity ratio between Na emission D_1 and D_2 lines can strongly varying between 0.5-0.9 depending on the physical condition of the emitting material (e.g. Nikaidou & Kawaguchi 1983; Slanger et al. 2005). The explanation of the second question may be that the phenomenon is temporary. This would not be unprecedented, since the cycle-to-cycle variation of RR Lyrae spectra is a known phenomenon (Chadid 2000). For more definite answers we need more spectroscopic time series observations.

6 SUMMARY

In this paper, we presented our results based on new photometric and spectroscopic time series for one of the brightest RRc stars T Sex. Our main findings are:

- From the Fourier analysis of the photometric data set of the *TESS* space telescope we obtained that the light curve of T Sex can be described by two independent frequencies: the frequency of the radial overtone pulsation f_1 and a frequency belongs to most probably an $l = 8$ non-radial mode pulsation. The speciality of T Sex Fourier spectrum is that the usual f_x frequency is not significant, only $0.5 f_x$ is observed. Such star has never been reported before. It is very rare (~ 3.6%, Netzel & Smolec 2019) and has only been detected in ground-based data so far, that the amplitude of $0.5 f_x$ is larger than that of f_x.
- In our time-resolved spectroscopic measurements, we showed a characteristic phase-dependent periodic distortion of the Hα line. This type of line profile variation is significantly different for RRab stars e.g. from the almost unchanged profiles seen at RR Lyr (Gillet et al. 2019). This type of profile change has not previously been published for RR Lyrae stars, only for other radial pulsators (Nardetto et al. 2008, 2013). The phenomenon is most likely caused by the relatively high macroturbulence velocity of T Sex (~ 15 – 20 km s^{-1}), which can be caused by convection. This plays a much larger role in the pulsation of RRc stars than in RRab pulsators.
- We discovered a phase-dependent line doubling of the Na D lines. This is the first case that such line doubling has been reported for overtone pulsating RR Lyrae stars. The possible explanation of the feature is the same as in the case of RR Lyr (Gillet et al. 2019): one of the line components come from the star and the other originate from the interstellar medium. This finding calls the attention to the fact that the characteristic velocity of the atmosphere of RR Lyrae star during pulsation is similar to the velocity of the ISM clouds in the wall of the Local Bubble. Thus, it is expected that most Galactic field RR Lyr stars will show similar Na D line doubling.
- At the phase $\phi = 0.438$, a definite emission peak was found on the red side of the sodium D_2 line, which forms a P Cyg profile with the absorption component. The appearance of P Cyg profiles in RR Lyrae spectra is usually associated with shock waves. Although no strong shock waves are expected for RRc stars, the appropriate phase of the detected event and the calculated shock wave velocity (~ 30 km s^{-1}) also suggest the appearance of a weak shock wave. Due to the single detection, the intrinsic nature of the phenomenon must be verified in the future.

ACKNOWLEDGEMENTS

This work was supported by the Hungarian National Research, Development and Innovation Office by the Grant NN-129075 and the Lendület Program of the Hungarian Academy of Sciences, project No. LP2018-7/2018. JMB thanks to Dr A. Moór and Dr R. Szabó for their valuable suggestions.

This work has made use of data from the European Space Agency (ESA) mission *Gaia* (`https://www.cosmos.esa.int/gaia`), processed by the *Gaia* Data Processing and Analysis Consortium (DPAC, `https://www.cosmos.esa.int/web/gaia/dpac/consortium`). Funding for the DPAC has been provided by national institutions, in particular the institutions participating in the *Gaia* Multilateral Agreement.

REFERENCES

Barnes, T. G., Moffett, T. J., Hawley, S. L., Slovak, M. H., Frueh, M. L. 1988, ApJS, 67, 403
Blanco-Cuaresma, S. 2019, MNRAS, 486, 2075
Blanco-Cuaresma, S., Soubiran, C., Heiter, U., Jofré, P. 2014, A&A, A111
Chadid, M. 2000, A&A, 359, 991
Chadid, M., Gillet, D. 1996, A&A, 308, 481
Chadid, M., Gillet, D. 1997, A&A, 319, 154
Chadid, M., Sneden, C., Preston, G. W. 2017, ApJ, 835, id.187
Chadid, M. et al. 2014, AJ, 148, id.88
Derekas, A. et al. 2017, MNRAS, 464, 1553
Dziembowski, W. A. 2016, in RRL2015 – High-Precision Studies of RR Lyrae Stars, eds. L. Szabados, R. Szabó, K. Kinemuchi, Comm. Konkoly Obs., 105, pp. 23-30.
Fokin, A. B., Gillet, D. 1997, A&A, 325, 1013
Frisch, P. C., Redfield, S., Slavin, J. D. 2011, ARA&A, 49, 237
Gaia Collaboration 2016, A&A, 595, A1
Gaia Collaboration 2018, A&A, 616, A1
Gautschy A. 2019, Astro-ph:1909.10444
Gillet, D. Crowe, R. A. 1988, A&A, 199, 242
Gillet, D. Fokin, A. B. 2014, A&A, 565, A73
Gillet, D., et al. 2017, A&A, 607, A51
Gillet, D., et al. 2019, A&A, 623, A109
Gontcharov, G. A. 2006, Astron. Letters, 32, 759
Gray, R. O., Corbally, C. J. 1994, AJ, 107, 742
Grevesse, N., Asplund, M., Sauval, A. J. 2007, Space Sci. Rev., 130, 105
Gustafsson, B., Edvardsson, B., Eriksson, K., Jørgensen, U. G., Nordlund, Å., Plez, B. 2008, A&A, 486, 951
Heiter, U. et al. 2015, A&A, 582, A49
Hill, S. J. 1972, ApJ, 178, 793
Hobbs, L. M. 1978, ApJ, 222, 491
Lenz, P., Breger, M. 2005, CoAst, 146, 53
Louistisserand, S., Büchner, A., Koutchmy, S., Lamy, Ph. 1987, A&AS, 68, 539
Karp, A. H. 1975, ApJ, 201, 641
Kollmeier, J. A. et al. 2013, ApJ, 775, id.57
Maintz, G. 2005, A&A, 442, 381
Molnár, L. et al. 2015, MNRAS, 452, 4283

Moskalik, P. 2013, in Stellar Pulsations: Impact of New Instrumentation and New Insights, eds: J. C. Suárez, R. Garrido, L. A. Balona & J. Christensen-Dalsgaard, Astrophys. Space Sci. Proc. 31, p. 103
Moskalik, P. et al. 2015, MNRAS, 447, 2348
Nardetto, N. et al. 2008, A&A, 489, 1235
Nardetto, N. et al. 2013, A&A, 553, A112
Netzel, H., Smolec, R. 2019, MNRAS, 487, 5584
Netzel, H., Smolec, R., Dziembowski, W. 2015, MNRAS, 451, L25
Nikaidou, Y., Kawaguchi, I. 1983, Sol. Phys., 84, 49
Jurcsik, J. et al. 2015, ApJS, 219, 25
Jurcsik, J. et al. 2017, MNRAS, 468, 1317
Points, S. D., Lauroesch, J. T., Meyer, D. M. 2004, PASP, 116, 801
Pojmański, G., Pilecki, B., Szczygieł, D. 2005, Acta Astron. 55, 275.
Preston, G. W. 2009, A&A, 507, 1621
Preston, G. W. 2011, AJ, 141, id.6
Preston, G. W., Paczyński, B. 1964, ApJ, 140, 181
Preston, G. W., Sneden, C., Chadid, M. Thompson, I. B., Shectman, S. A. 2019, AJ, 157, id.153
Prudil Z., Smolec R., Skarka M., Netzel H. 2017, MNRAS, 465, 4074
Rebollido, I. et al. 2018, A&A, 614, A3
Redfield, S. 2007, ApJ, 656, L97
Redfield, S., Kessler-Silacci, J. E., Cieza, L. A. 2007, ApJ, 661, 944
Ricker, G. R. et al. 2015, J. Astron. Tel. Instr. Sys., 1, id.014003
Rudolf, N., Günther, H. M., Schneider, P. C., Schmitt, J. H. M. M. 2016, A&A, 585, A113
Sneden, C., Preston, G. W., Chadid, M., Adamów, M. 2017, ApJ, 848, id.68
Schrijvers, C., Telting, J. H., Aerts, C., Ruymaekers, E., Henrichs, H. F 1997, A&AS, 121, 343
Schrijvers, C., Telting, J. H. 1999, A&A, 342, 453
Schwarzschild, M. 1952, Transactions of the IAU VIII, ed., P. TH. Oosterhoff (Cambridge: Cambridge University Press), 8, 811
Slanger, T. G. et al. 2005, J. Geophy. Res., 110, D23302
Sódor, Á., Skarka, M., Liška, J, Bognár, Zs. 2017, MNRAS, 465, L1
Szabó, R. et al. 2014, A&A, 570, A100
Stanford, R. F. 1949, ApJ, 109, 208
Struve, O., Blaauw, A. 1948, ApJ, 108, 60
Tift, W. G., Smith, H. J. 1958, ApJ, 127, 591
Telting, J. H., Schrijvers, C. 1997, A&A, 317, 723
Tody, D. 1986, in Proc. SPIE Instrumentation in Astronomy VI, ed. D. L. Crawford, p. 627
Tody, D. 1993, in Astronomical Data Analysis Software and Systems II, eds. R. J. Hanisch, R. J. V. Brissenden, & J. Barnes, ASP Conference Ser., Vol 52, p. 173
Vergely, J.-L., Valette, B., Lallement, R., Raimond, S. 2010, A&A, 518, A31
Welsh, B. Y., Lallement, R., Vergely, J.-L., Raimond, S. 2010, A&A, 510, A54

This paper has been typeset from a TEX/LATEX file prepared by the author.